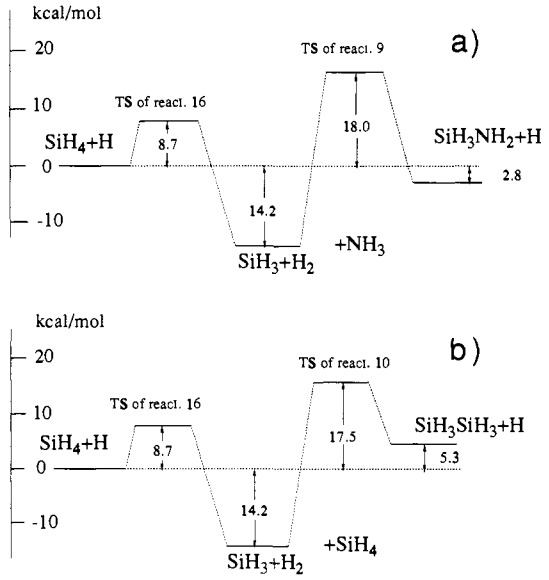

Figure 3. Energy diagrams for (a) chain I and (b) chain II.

dothermic. The ΔH_{exptl} values for chain I and II are consistent with the corresponding ΔH values (See Figure 3).

Some side chain reactions can be derived from the combination of basic reactions we discussed previously, e.g., reactions 17 and 14 (Si-N bond formation chain). However, all such side chain reactions include the formation of the particularly unstable NH_2 radical, and hence their contribution to the Si-N bond formation is likely negligible.

The radical chain reaction mechanism I gives the most reasonable explanation for selective Si-N bond formation and the lowest energy surface for the bond formation compared with other reaction mechanisms.

Conclusions

The following new points emerge from this study.

1. The SiH_3 radical is confirmed to be an extraordinarily stable reactive species in the silane CVD system. This is consistent with the observation of a high concentration of SiH_3 radicals in actual CVD experiments.[17,18]

2. As a method for the Si-N bond formations, the radical substitution reactions turn out to be more favorable energetically than any other bond formation reactions, namely, the silylene insertion or the direct bond formation, assuming that the radical substitution reaction is more likely to occur than the recombination. Under the conditions of real CVD experiments,[1,5] this assumption seems to be satisfied.

3. In the reaction of silane and ammonia, the order of reactivity of bond formation is predicted to be Si-N > Si-Si ≫ N-N. In the CVD experiments,[1,5] it has been observed that the formation of Si-N and Si-Si bonds in the heated gas mixture of silane and ammonia occurs under comparable reaction conditions and that the N-N bond formation is unlikely to occur. These are consistent with the theoretical prediction.

In the case of the laser CVD process of silicon ceramics, the surface reaction is said to play a role.[3,6] Evaluating such a complex surface reaction is beyond the scope of the present study. This present study represents a preliminary attempt toward a better understanding of the complex CVD reaction mechanism.

Acknowledgment. This work was supported by a Grant-in-Aid for Scientific Research from the Ministry of Education, Science and Culture of Japan, for which we express our gratitude. We also thank the Data Processing Center of Kyoto University for a grant of time on the FACOM M-780 and VP-2600 computers, and the Computer Center of the Institute for Molecular Science for time on the HITAC M-680H and S-820 computers.

Registry No. Si_3N_4, 12033-89-5; SiH_3, 13765-44-1; SiH_4, 7803-62-5; NH_3, 7664-41-7; H, 12385-13-6.

Σ Metathesis Reactions Involving Group 3 and 13 Metals. $Cl_2MH + H_2$ and $Cl_2MCH_3 + CH_4$, M = Al and Sc

A. K. Rappé*,† and T. H. Upton‡

Contribution from the Department of Chemistry, Colorado State University, Fort Collins, Colorado 80523, and Products Research Division, Exxon Research and Engineering, Linden, New Jersey 07036. *Received March 6, 1992*

Abstract: Correlated ab initio theoretical calculations at the valence double zeta plus polarization level are used to study the degenerate exchange processes involving metal-hydrogen, metal-carbon, hydrogen-hydrogen, and carbon-hydrogen σ bonds observed for early transition metal complexes (groups 3 and 4). In agreement with Rooney's hypothesis, we find that an empty p orbital can rehybridize with a bonding p orbital to permit four-center 2 + 2 reactions to occur with relatively low activation energies for aluminum-hydrogen and aluminum-carbon σ bonds. However, the greater directionality of a d orbital permits the reactions to occur with substantially lower barriers for the transition metal cases (for hydrogen exchange, the Al barrier is 32.2 kcal/mol higher than for Sc; for methane exchange, the Al barrier is 33.7 kcal/mol higher than for Sc). Further, we present computational evidence for the hypothesis that metal fragment orbitals can be tuned to either stabilize transition states of preferred reactions or destabilize transition states for pathways that are not desired. We calculate a barrier for methane exchange of 28.0 kcal/mol for $Cl_2Sc(CH_3) + CH_4$. Further, we determine the methyl plus methane exchange process to occur with a barrier of less than 25.1 kcal/mol.

I. Introduction

In the past several years it has become apparent that early transition metal complexes possess unique reactivity patterns[1-3] that have been attributed to quite small activation energetics for four-center 2 + 2 reactions. Several members of this class of reactions have been studied theoretically,[4-9] and these studies led us[8,9] to propose (as an extension of the orbital phase continuity principle[4,8,10]) that the essential electronic factor was the presence

† Colorado State University.
‡ Exxon Research and Engineering.

(1) (a) Thompson, M. E.; Bercaw, J. E. *Pure Appl. Chem.* **1984**, *56*, 1-11. (b) Bercaw, J. E.; Davies, D. L.; Wolczanski, P. T. *Organometallics* **1986**, *5*, 443-450. (c) Thompson, M. E.; Baxter, S. M.; Bulls, A. R.; Burger, B. J.; Nolan, M. C.; Santarsiero, B. D.; Schaefer, W. P.; Bercaw, J. E. *J. Am. Chem. Soc.* **1987**, *109*, 203-219. (d) Bunel, E.; Burger, B. J.; Bercaw, J. E. *J. Am. Chem. Soc.* **1988**, *110*, 976-978.

0002-7863/92/1514-7507$03.00/0

of an energetically accessible empty d orbital on the metal center. Our theoretical results did not exclude the possibility of p orbitals playing the same role, and we presently suggest that group 13 metals such as Al should undergo the same reactions. Rooney[11] has proposed that four-center 2 + 2 reactions occur at aluminum centers and has suggested a related zwitterionic mechanism for aluminum based reactions. Studies of the addition of ethylene and acetylene across an aluminum–hydride bond have been reported by Sakai.[12]

In this paper we compare the valence orbitals for the transition states and activation energetics for a pair of degenerate metathesis reactions for both M = Sc (group 3) and M = Al (group 13), L = Cl. Both (1) and (2) are experimentally observed[1] for M = Sc and L = Cp* (pentamethylcyclopentadienyl) and have been termed σ-bond metathesis processes.[1]

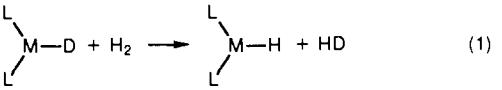
(1)

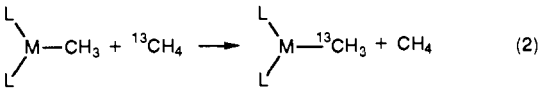
(2)

We first discuss, in section II, the Pauli principle constraints on four-center 2 + 2 reactions, the general electronic reorganization that we have found to be common to all four-center 2 + 2 reactions containing a transition metal d orbital, and an analogous molecular orbital description of the same electronic reorganization. A comparison of the calculated results for reactions 1 and 2 for group 3 (Sc) and 13 (Al) analogues is presented in section III. In section IV the overall results obtained to date are used to develop a general picture of reactivity at high-valent metal centers. The conclusions are given in section V and the theoretical details are given in section VI.

II. General Four-Center 2 + 2 Electronic Reorganization

By way of review we consider first the H/D exchange process for the electronically degenerate H_2 plus D_2 reaction. This

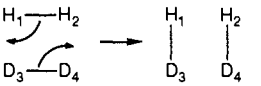
(3)

reaction is useful for illustrating how the constraints of the Pauli principle determine the evolution of one-electron states from reactants to the transition state in a reaction where σ orbitals are involved.[4,8-10] We presume, conceptually, the reaction to begin from an interaction geometry in which the hydrogen H–H σ bonds are parallel to one another though changes in geometry will not change the underlying physics.

The reaction limit wave functions may be represented as

$$\Psi(H_2 + D_2) = {}^1A_{1g} = A\{\sigma_1\sigma_2(\alpha\beta - \beta\alpha)\sigma_3\sigma_4(\alpha\beta - \beta\alpha)\} \quad (4a)$$

$$\Psi(HD + DH) = {}^1A_{1g} = A\{\sigma_1\sigma_3(\alpha\beta - \beta\alpha)\sigma_2\sigma_4(\alpha\beta - \beta\alpha)\} \quad (4b)$$

where the subscripts identify the atomic locations of the orbitals. The σ_i orbitals are 1s orbitals on the hydrogens that are coupled into two singlet pairs (bonds) to produce the two hydrogen σ bonds. For the geometry chosen here, bonds are formed between the first two and last two orbitals listed in each wave function. For the total wave function to be an eigenfunction of spin, each of the first two orbitals is then coupled to each of the last two orbitals via a predominantly triplet ($^3/_4$ triplet + $^1/_4$ singlet) or "antibonding" interaction. A schematic display of these interactions and the orbital positions is as follows:


(5a)


(5b)

The solid line represents a singlet coupling between the orbitals connected by it, and the dotted line denotes the partial triplet coupling. The Pauli principle, in requiring a wave function to be antisymmetric, allows two "bonding" interactions in each wave function (the solid lines) and necessitates two additional partial "antibonding" interactions (the dotted lines). The "antibonding" interactions vanish as the molecule–molecule separation increases.

As the atoms move from either reactant or product position to the transition state, the four hydrogen atoms form a rectangle and then a square. The reactant (4a) and product (4b) states are the same energy at this point, but neither is appropriate to accurately describe the transition-state wave function. The wave function may, however, be approximately represented[13] as a superposition of these two states

$$\Psi(TS)_\pm = N_\pm\{\Psi(H_2 + D_2) \pm \Psi(HD + DH)\} \quad (6)$$

where $N_\pm$ is the appropriate normalization and the two possible states correspond to symmetric and antisymmetric superposition. A more complete expression would include ionic contributions, but for this qualitative description the above is sufficient. Interactions in these two wave functions become

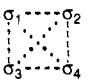
(7a)

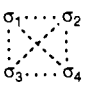
(7b)

Orbitals that are triplet coupled are connected by the dotted lines (as before). The remaining pairs of orbitals are primarily singlet coupled and are connected to each other by dashed lines. The wave function Ψ_+, (7a), maximizes the separation between triplet-coupled orbitals while maximizing the overlap between partially singlet-coupled (bonding) orbitals and is thus preferred over Ψ_-, (7b), where the reverse occurs. The lowest transition-state wave function will be best represented by the symmetric superposition, Ψ_+. It provides the best opportunity to maintain bond order between bonded centers. the appearance of a low-energy transition state (i.e., small barrier) will be largely a result of how well these

(2) Watson, P. L. *J. Am. Chem. Soc.* **1982**, *104*, 337–339. Watson, P. L. *J. Chem. Soc., Chem. Commun.* **1983**, 276–277. Watson, P. L. *J. Am. Chem. Soc.* **1983**, *105*, 6491–6493. Watson, P. L.; Parshall, G. W. *Acc. Chem. Res.* **1985**, *18*, 51–56.

(3) Casey, C. P.; Neumann, S. M. *J. Am. Chem. Soc.* **1977**, *99*, 1651–1652. Wengrovius, J. H.; Schrock, R. R.; Churchill, M. R.; Wasserman, H. J. *J. Am. Chem. Soc.* **1982**, *104*, 1739–1740. Chamberlain, L. R.; Rothwell, I. P.; Huffman, J. C. *J. Am. Chem. Soc.* **1982**, *104*, 7338–7340. Chamberlain, L. R.; Rothwell, A. P.; Rothwell, I. P. *Ibid.* **1984**, *106*, 1847–1848. Chamberlain, L. R.; Rothwell, I. P.; Huffman, J. C. *Ibid.* **1986**, *108*, 1502–1509.

(4) Steigerwald, M. L.; Goddard, W. A. *J. Am. Chem. Soc.* **1984**, *106*, 308–311.

(5) Fujimoto, H.; Yamasaki, T.; Mizutani, H.; Koga, N. *J. Am. Chem. Soc.* **1985**, *107*, 6157–6161.

(6) Sakaki, S.; Kitaura, K.; Morokuma, K.; Ohkubo, K. *J. Am. Chem. Soc.* **1983**, *105*, 2280. Koga, N.; Obara, S.; Kitaura, K.; Morokuma, K. *J. Am. Chem. Soc.* **1985**, *107*, 7109–7116. Koga, N.; Morokuma, K. *J. Am. Chem. Soc.* **1985**, *107*, 7230. Koga, N.; Morokuma, K. *J. Am. Chem. Soc.* **1986**, *108*, 6136. Koga, N.; Daniel, C.; Han, J.; Fu, X. Y.; Morokuma, K. *J. Am. Chem. Soc.* **1987**, *109*, 3455. Koga, N.; Jin, S. Q.; Morokuma, K. *J. Am. Chem. Soc.* **1988**, *110*, 3417. Daniel, C.; Koga, N.; Han, J.; Fu, X. Y.; Morokuma, K. *J. Am. Chem. Soc.* **1988**, *110*, 3773. Koga, N.; Morokuma, K. *Chem. Rev.* **1991**, *91*, 823.

(7) Rabaâ, H.; Sailard, J.-Y.; Hoffmann, R. *J. Am. Chem. Soc.* **1986**, *108*, 4327–4333.

(8) Upton, T. H. *J. Am. Chem. Soc.* **1984**, *106*, 1561–1571.

(9) (a) Rappé, A. K.; Upton, T. H. *Organometallics* **1984**, *3*, 1440–1442. (b) Upton, T. H.; Rappé, A. K. *J. Am. Chem. Soc.* **1985**, *107*, 1206–1218. (c) Rappé, A. K. *Organometallics* **1987**, *6*, 354–357. (d) Rappé, A. K. *Organometallics* **1990**, *9*, 466.

(10) Goddard, W. A. *J. Am. Chem. Soc.* **1970**, *92*, 7520–7521. Goddard, W. A.; Ladner, R. C. *Ibid.* **1971**, *93*, 6750–6756. Goddard, W. A. *Ibid.* **1972**, *94*, 793–807.

(11) Rooney, John J. *J. Chem. Soc., Chem. Commun.* **1983**, 1301–2. Hamilton, James G.; Rooney, John J. *J. Chem. Soc., Faraday Trans.* **1984**, *80*, 129–133. Rooney, J. J. *J. Mol. Catal.* **1985**, *31*, 147–159.

(12) Sakai, S. *J. Phys. Chem.* **1991**, *95*, 175, 7089.

(13) Bernardi, R.; Robb, M. A. *J. Am. Chem. Soc.* **1984**, *106*, 54.

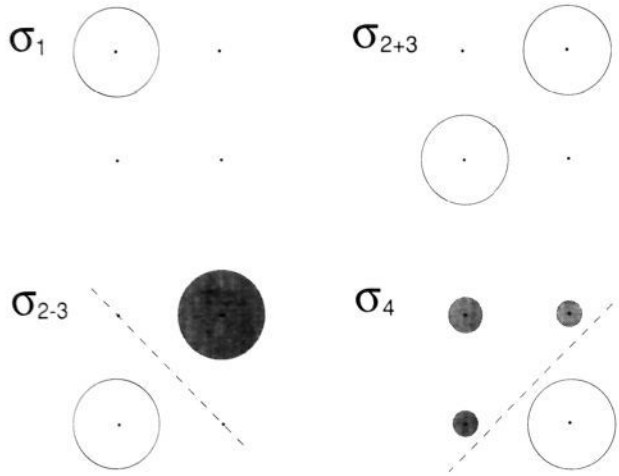

Figure 1. Orbital diagrams for the interaction of H_2 with D_2 near the saddle point.

specific orbitals are able to maximize the strength of the "bonding" interactions while minimizing the destabilization resulting from the necessary triplet interactions.

In the approach toward the transition state, the four one-electron orbitals involved in the bonds delocalize onto different centers. The driving force for this delocalization is the presence of the triplet interactions in the transition-state wave function (dotted lines in (7)). These triplet interactions are repulsive, and the Pauli principle forces the pair of orbitals involved in each interaction (connected by dotted lines) to be orthogonal to one another. For this symmetric superposition of equivalent or nearly equivalent wave functions, the orthogonality requirement is *the* most important effect of the superposition process and the source of the energetic barrier. This orthogonality condition is best satisfied by the formation of delocalized bonding–antibonding orbital pairs.

To see the consequences of the orthogonality condition imposed formation of delocalized bonding–antibonding orbital pairs, we will consider each of the four one-electron orbitals separately. We will consider σ_1, the first one-electron orbital of the bonding (first) pair to be minimally perturbed from its original shape (see Figure 1, σ_1). In reality all four orbitals will be perturbed in response to the orthogonality constraint, but we are perturbing them sequentially here in order to emphasize the essential restriction in orbital shapes dictated by the Pauli principle orthogonality constraint. The second one-electron orbital of the bonding (first) pair, σ_{2+3}, symmetrically delocalizes from center 2 onto center 3, retaining overlap with σ_1 (see Figure 1, σ_{2+3}). Both one-electron orbitals of the second pair must remain orthogonal to the first pair (in reality both pairs are perturbed in response to the orthogonality constraint; we are conceptually simplifying the situation here). If we focus first on what happens to σ_3, we see that since σ_{2+3} delocalizes onto center 3 symmetrically, σ_3 must delocalize onto center 2 antisymmetrically in order remain orthogonal to σ_{2+3}. Thus σ_3 builds in a nodal surface passing through centers 1 and 4 (see Figure 1, σ_{2-3}). The orbital originally on center 4, σ_4, must also become orthogonal to σ_1 and σ_{2+3}, but it cannot do so by building in a node at center 4 since σ_4 is an s orbital centered on center 4. The orbital σ_4 can become orthogonal to the first bond pair by building in antibonding combinations of the functions σ_1 and σ_{2+3} (see Figure 1, σ_4). At this point the second pair is orthogonal to the first pair; the Pauli principle is satisfied, but σ_{2-3} and σ_4 are now orthogonal. In terms of these new delocalized orbitals, the transition-state wave function Ψ_+ becomes

$$\Psi_+ = A\{\sigma_1\sigma_{2+3}(\alpha\beta - \beta\alpha)\sigma_{2-3}\sigma_4(\alpha\beta - \beta\alpha)\} \qquad (8)$$

Overlap between σ_1 and σ_{2+3} is retained so the bond order of the transition state is reduced from two in the reactants or products to one in the transition state. The energy of the transition state is high, and the reaction is forbidden.

If the 1s hydrogen orbital σ_4 of the above discussion is replaced by an orbital with a node passing through center 4 such as a p_π or d_π orbital, the overlap between σ_4 and σ_{2-3} would be retained and the bond order of the transition state would not drop below two. The energy of the transition state would now not necessarily be high, and the reaction could be allowed.

Generalized Description. In general, the orbital reorganization found to be common to theoretical studies of metal containing four-center 2 + 2 reactions[4-9] is as follows:

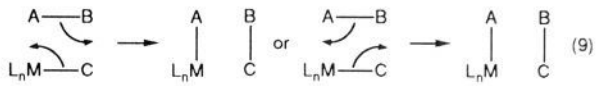

The common features observed in the transition-state wave functions (consistent with the above discussion for H_2 plus D_2) are (1) that two active bond pairs smoothly move from the reactant description to the product description and (2) that two one-electron orbitals remain on their original centers (either M and B or A and C), and the remaining two one-electron orbitals delocalize onto alternate centers. If "symmetry" (e.g., H_2 plus D_2, ethylene plus ethylene, or even ethylene plus formaldehyde) precludes this localization, the reactions have a high activation energy.[9a,b] That is, if both directions for electron flow are nearly equivalent, localization will not be possible and the Pauli principle dictated orthogonality constraints must be satisfied by forming an antibonding pair. If there is a significant energy difference between the AB bond and the MC bond, then the stronger bond (usually AB) is transformed with minimal orthogonality constraints. The weaker bond (usually between M and C) builds in Pauli principle induced orthogonality constraints to the AB (reactant) or BC (product) bonding orbital. If one of the orbitals (the one on M) involved in the weaker bond can rehybridize to retain overlap with its bonding partner while still being orthogonal to the stronger bond, the reaction will occur with a low barrier. The requirement for this rehybridization to occur with low energy is that there be an energetically accessible empty orbital of the correct shape to rehybridize with the one-electron orbital on center M. The cases studied to date[4-9] have considered systems with occupied d_σ and d_π orbitals. There is, however, no reason to exclude an occupied p_σ orbital from rehybridizing with an empty p orbital. For both the scandium and aluminum systems discussed below, we find the above-described one-electron orbital reorganization for both (1) and (2). A comparison of the transition-state valence orbitals, geometries, and activation energetics is provided below in section III for both the hydrogen exchange reaction (1) and the degenerate σ metathesis reaction (2).

Molecular Orbital Description of Electronic Reorganization. The important electronic reorganization events discussed above in terms of individual one-electron orbitals can also be cast in terms of doubly occupied molecular orbitals (see also ref 14). The principal difference between the analyses is in the occupation of the fragment orbitals.

Consider first the interaction between H_2 and D (or D^-). As shown in Figure 2, the two molecular orbitals (or the two natural orbitals of a GVB analysis) of H_2 (centers A and B in the discussion in section II above) on the left interact with the atomic orbital of D (or D^-) on the right (center C in the above discussion) to form a set of three orbitals which at the symmetric saddle point are bonding, nonbonding, and antibonding (the lowest and highest are the two natural orbitals of a GVB analysis). Addition of the fourth center (center M in the discussion above) (and fourth orbital) to the molecular orbital diagram in the center of Figure 2 completes the molecular orbital analysis of a four-center 2 + 2 reaction. This fourth orbital is initially bonded to (or stabilizes in the case of D^-) the atomic orbital of D (or D^-) for the reactants (as shown in Figure 3a). As shown in Figure 3b, if the nonbonding orbital localized on centers A and C can be stabilized through interaction with this fourth orbital (on center M), the 2 + 2 reaction will proceed with low barrier (bonding will be retained throughout the reaction). If the fourth orbital is of the wrong shape (symmetry) to interact (overlap) with the nonbonding orbital at the saddle point, then the 2 + 2 reaction will not proceed

(14) Saillard, J.-Y.; Hoffmann, R. *J. Am. Chem. Soc.* **1984**, *106*, 2006.

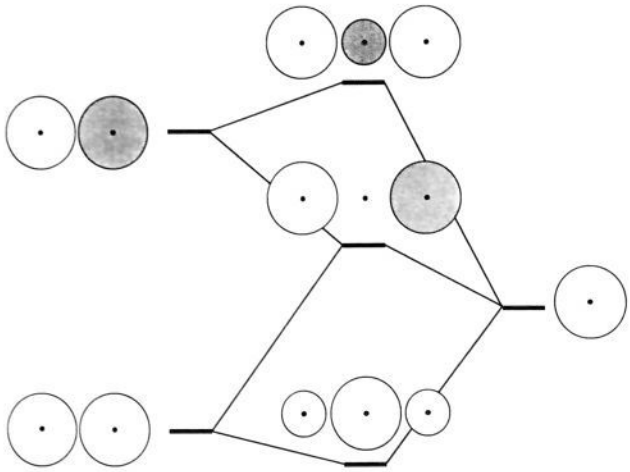

Figure 2. Orbital correlation diagram for the interaction of H_2 with D (*or* D^-).

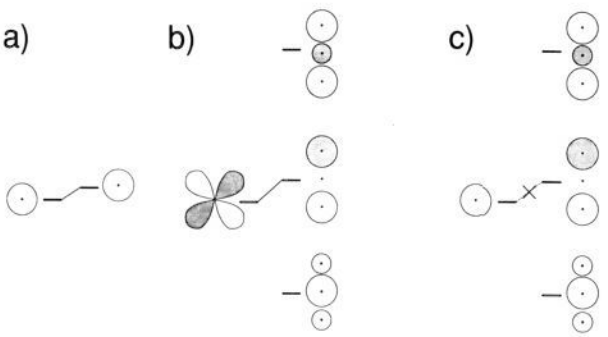

Figure 3. Orbital correlation diagrams for the interaction of a fourth center with the orbitals presented in Figure 1: (a) the interaction of the fourth orbital with the orbital on D in the reactants; (b) the interaction of the fourth orbital with the nonbonding orbital at the saddle point (a d_π orbital is shown; a p_π orbital would have the same effective shape); (c) the interaction of the fourth orbital with the nonbonding orbital at the saddle point (this s (or σ) orbital does not have the correct shape to overlap with the nonbonding orbital as indicated by the × in the interaction diagram).

with a low barrier (as shown in Figure 3c). The initial bond between the fourth orbital and the atomic orbital of the D will have been broken at the saddle point, and the reaction will have a barrier comparable to the energy of this bond. This fragment orbital analysis can be generalized to any 2 + 2 process involving two bond pairs. As discussed previously,[4,8-10] the s orbital of hydrogen cannot fulfill the role of the fourth orbital, and hence the barrier for H_2 plus D_2 is high. In addition, the p_π orbital of carbon in ethylene is incapable of adopting the correct shape, and hence the barrier for ethylene plus ethylene is high. As discussed previously,[4,9] the d_π orbital of a transition metal center can adopt the correct shape, and hence the barrier for the 2 + 2 reaction in olefin metathesis is small. As discussed above, a p_π orbital on aluminum can also adopt the correct shape, and as discussed below reactions at aluminum are calculated to have relatively small barriers (smaller than the associated radical process involving bond breakage).

III. Results

In order to probe the generality of the overall scheme outlined above, we have studied a pair of degenerate processes (1) and (2) for two metals (Al and Sc) as well as the three-electron parent reactions H_2 plus D and CH_3 plus $^{13}CH_4$. Below in subsection A we sketch the electronic reorganizations that occur in the three-electron parent reactions. In subsection B we compare our computational results for the hydrogen exchange reaction (1) for aluminum and scandium. In subsection C we compare our computational results for the methane exchange (σ metathesis) reaction (2) for aluminum and scandium.

A. H_2 + D and CH_3 + $^{13}CH_4$. The parent three-electron exchange reaction involving H_2 + D is certainly the most thoroughly and accurately studied chemical reaction.[15,16] The Generalized Valence Bond description of the electronic reorganization found in H_2 plus D was first published by Ladner and Goddard in 1972.[15] The most reliable potential surface to date was calculated by Liu.[16] Briefly, at the transition state the H_3 three hydrogen atom electrons are arranged into a symmetrically delocalized singlet coupled pair (originally the H_2 bond pair) (see Figure 4, a and b) and a radical electron in an antisymmetric orbital orthogonal to the bond pair (see Figure 4c). The electronic barrier for the exchange process is due to the increase in kinetic energy associated with the nodal plane introduced to account for the Pauli principle orthogonality constraint. That the reaction occurs with only a 9.86-kcal/mol classical barrier[16] is due to the symmetric delocalization afforded the singlet coupled bond pair. With the present wave function and basis set we obtain a barrier height of 14.4 kcal/mol and an H–H distance of 0.911 Å (accurate calculations[16] yield a barrier of 9.86 kcal/mol and an H–H distance of 0.931 Å). All radical plus bond reactions are merely variants of this process.[17-22] The active orbitals for the transition state of the analogous degenerate methyl plus methane reaction are given in Figure 4, d–f, and are quite similar to the H_2 + H case. That is, there is a symmetrically delocalized singlet pair and an antisymmetrically delocalized radical orbital. Further, in both cases a single one-electron orbital of the bond pair moves; the second one-electron orbital stays on its original (hydrogen) center.

The barrier for the methyl plus methane exchange process is calculated to be 25.1 kcal/mol, 10.7 kcal/mol above the H_2 + H barrier (calculated with the same methodology) but still rather small. The coordinates for the transition state are given in Table Ia, and the major bond distances and bond angles are given in Table IIa. Previous theoretical results[17] using at least a valence double-ζ plus polarization function basis yielded C–H distances of 1.335 Å (CI) and 1.356 Å (UHF) in good agreement with the present RHF optimized distance of 1.337 Å. Barrier heights of 29 kcal/mol (UHF) and 25 kcal/mol (SDCI) were obtained. As with the H_2 + H result above, there should be an overestimation of the barrier height of at least 4.5 kcal/mol, leading to an estimated barrier of ~20 kcal/mol for the CH_3 + CH_4 exchange process. Experimental estimates place the barrier near 15 kcal/mol.[23]

B. Hydrogen Exchange. As discussed in section II above, we assert that the reaction of X_2MH + H_2 is merely a minor perturbation on the H + H_2 reaction. That is, the additional orbital and electron provided to the reaction by L_2M interacts with the

(15) Goddard, W. A.; Ladner, R. C. *Int. J. Quantum Chem., Symp.* **1969**, *3*, 63–66.
(16) Liu, B. *J. Chem. Phys.* **1984**, *80*, 581. Blomberg, M. R. A.; Liu, B. *Ibid.* **1985**, *82*, 1050–1051 and references therein.
(17) Wildman, T. A. *Chem. Phys. Lett.* **1986**, *126*, 325. Fox, G. L.; Schlegel, H. B. *J. Phys. Chem.* **1992**, *96*, 298.
(18) Walch, S. P. *J. Chem. Phys.* **1980**, *72*, 4932–4940. Dunning, T. H. *J. Chem. Phys.* **1980**, *73*, 2304–2309. Harding, L. B.; Wagner, A. F.; Bowman, J. M.; Schatz, G. C.; Christoffel, K. *J. Phys. Chem.* **1982**, *86*, 4312–4327. Harding, L. B.; Schatz, G. C. *J. Chem. Phys.* **1982**, *76*, 4296–4297. Dunning, T. H.; Harding, L. B.; Bair, R. A.; Eades, R. A.; Shepard, R. L. *J. Phys. Chem.* **1986**, *90*, 344–356 and references therein.
(19) Schlegel, H. B. *J. Phys. Chem.* **1982**, *86*, 4878–4882. Schlegel, H. B.; Bhalla, K. C.; Hase, W. L. *Ibid.* **1982**, *86*, 4883–4888. Schlegel, H. B.; Sosa, C. *Ibid.* **1984**, *88*, 1141–1145. Sosa, C.; Schlegel, H. B. *J. Am. Chem. Soc.* **1987**, *109*, 4193. Sosa, C.; Schlegel, H. B. *J. Am. Chem. Soc.* **1987**, *109*, 7007. Gonzalez, C.; Sosa, C.; Schlegel, N. B. *J. Phys. Chem.* **1989**, *93*, 2435. Gonzalez, C.; McDouall, J. J. W.; Schlegel, H. B. *J. Phys. Chem.* **1990**, *94*, 7467.
(20) Houk, K. N.; Paddon-Row, M. N.; Spellmeyer, D. C.; Rondan, N. G.; Nagase, S. *J. Org. Chem.* **1986**, *51*, 2874–2879. Dorigo, A.; Houk, K. N. *J. Org. Chem.* **1988**, *53*, 1650. Dorigo, A. E.; McCarrick, M. A.; Loncharich, R. J.; Houk, K. N. *J. Am. Chem. Soc.* **1990**, *112*, 7508.
(21) Arnaud, R.; Barone, V.; Olivella, S.; Sole, A. *Chem. Phys. Lett.* **1985**, *118*, 573–579. Arnaud, R. *New J. Chem.* **1991**, *15*, 615.
(22) Nagase, S.; Kern, C. W. *J. Am. Chem. Soc.* **1979**, *101*, 2544–2549. Nagase, S.; Kern, C. W. *J. Am. Chem. Soc.* **1980**, *102*, 4513–4515.
(23) Creak, G. A.; Dainton, F. S.; Ivin, K. J. *Trans. Faraday Soc.* **1962**, *58*, 328.

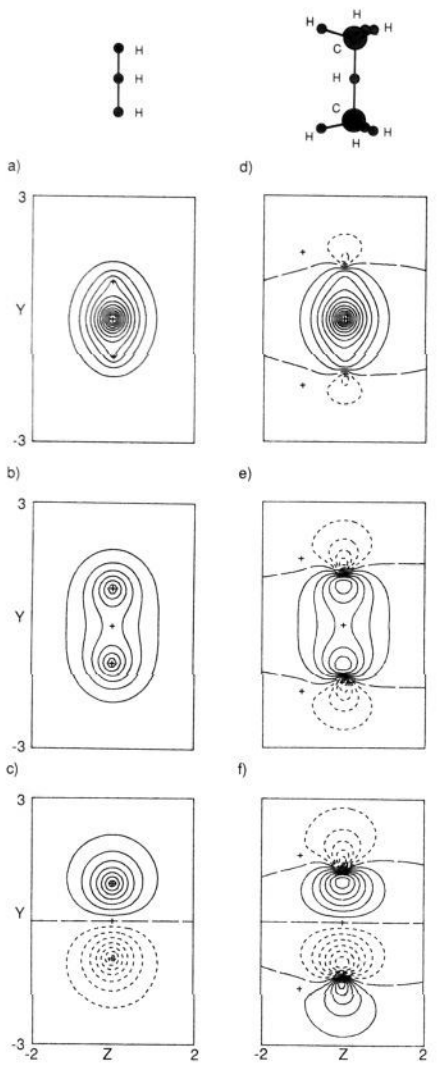

Figure 4. Contour plots of the GVB orbitals defining the one-electron orbitals of the H_2 + H transition state (a–c) and the CH_3 + CH_4 transition state (d–f). The plotting plane for a–c contains all three hydrogens. The plotting plane for d–f contains the two carbons and the bridging hydrogen. The solid contours define positive orbital amplitude (spaced 0.05 au), the dashed contours define negative orbital amplitude, and the long dashed lines define nodal lines: (a) the H_b σ one-electron orbital (of the singlet coupled pair), (b) the symmetrically delocalized σ one-electron orbital (of the singlet coupled pair), (c) the antisymmetrically delocalized radical σ one-electron orbital, (d) the H_b σ one-electron orbital (of the singlet coupled pair) of the methane exchange reaction; (e) the symmetrically delocalized σ one-electron orbital (of the singlet coupled pair) of the methane exchange reaction, and (f) the antisymmetrically delocalized radical σ one-electron orbital of the methane exchange reaction.

radical orbital to form a singlet coupled pair (bond). In the reactant (and product) the hydrogen atom radical orbital is bonded to the orbital and electron provided by L_2M, and at the transition state the antisymmetric radical orbital is bonded to L_2M. If the L_2M orbital can rehybridize, the reaction will occur with a low barrier because overlap will be retained with the radical orbital from the three-electron system. If the L_2M orbital cannot rehybridize (i.e., if M = C and all four valence orbitals are occupied, the usual circumstance for M=C), then the bond between L_2M and the radical orbital will be broken at the transition state and the reaction will have a high barrier. For cases where the L_2M orbital can rehybridize, one obvious difference between the main group and transition metal reactions is the better directionality afforded the transition metal d orbital. We find that for the hydrogen exchange reaction (1), for both the scandium and aluminum systems the three predominantly hydrogen orbitals are

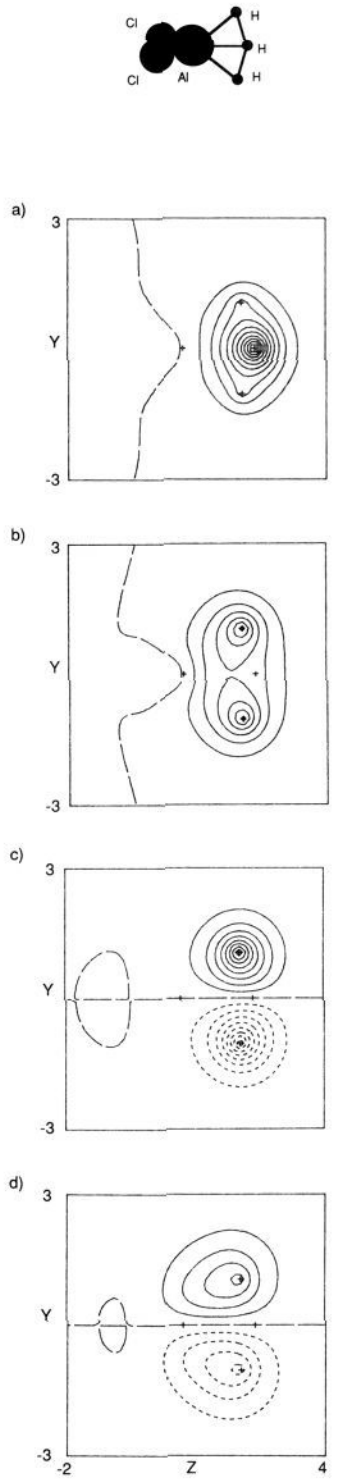

Figure 5. Contour plots of the GVB orbitals defining the one-electron orbitals of the H_2 + Cl_2AlH transition state. The plotting plane contains all three hydrogens and aluminum. The solid contours define positive orbital amplitude (spaced 0.05 au), the dashed contours define negative orbital amplitude, and the long dashed lines define nodal lines: (a) the H_b σ one-electron orbital (of the first singlet coupled pair), (b) the symmetrically delocalized σ one-electron orbital (of the first singlet coupled pair), (c) the antisymmetrically delocalized σ one-electron orbital (of the second singlet coupled pair), (d) the antisymmetrically delocalized σ one-electron orbital (of the second singlet coupled pair) more delocalized onto Al.

virtually identical with the H_3 three-electron system discussed above (see Figures 4, 5, , and 6 a–c). The better directionality of the d orbital is apparent from a comparison of Figures 5d and

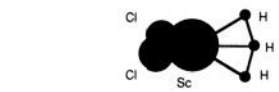

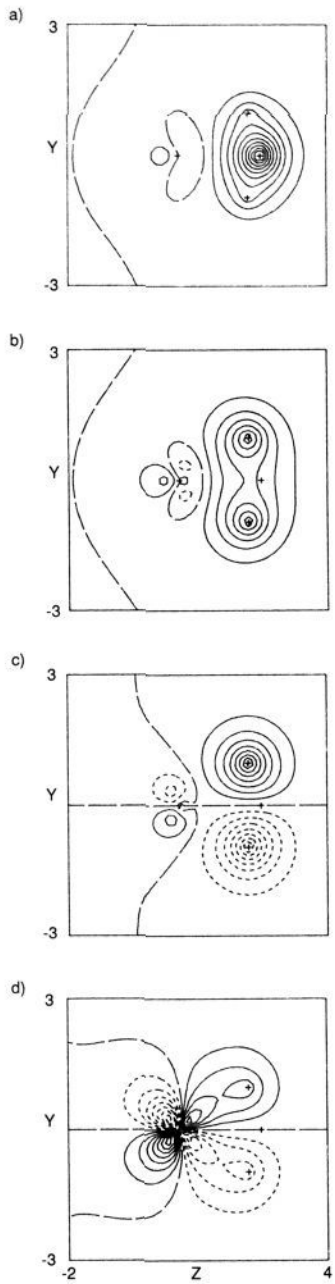

Figure 6. Contour plots of the GVB orbitals defining the one-electron orbitals of the $H_2 + Cl_2ScH$ transition state. The plotting plane contains all three hydrogens and scandium. The solid contours define positive orbital amplitude (spaced 0.05 au), the dashed contours define negative orbital amplitude, and the long dashed lines define nodal lines: (a) the H_b σ one-electron orbital (of the first singlet coupled pair), (b) the symmetrically delocalized σ one-electron orbital (of the first singlet coupled pair), (c) the antisymmetrically delocalized σ one-electron orbital (of the second singlet coupled pair), (d) the antisymmetrically delocalized σ one-electron orbital (of the second singlet coupled pair) more localized on Sc.

6d). The orbitals plotted in Figure 6 are virtually identical with those reported previously by Steigerwald and Goddard[4] for this precise system.

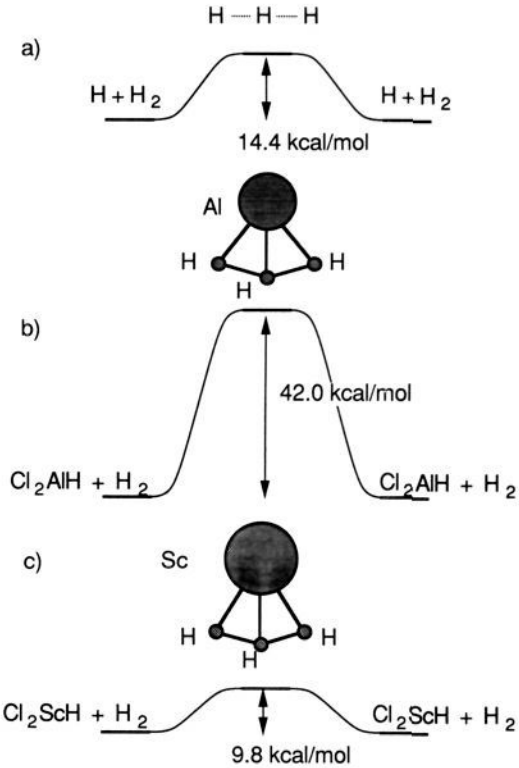

Figure 7. The reaction energy diagrams for hydrogen exchange processes: (a) the free $H_2 + H$ case, (b) the $Cl_2AlH + H_2$ case, (c) the $Cl_2ScH + H_2$ case. The energies are obtained from the CI calculations.

As expected from the comparison of valence orbitals, the geometries for the three transition states are quite similar. The H–H distances of 1.07 Å and 1.01 Å for Al and Sc, respectively, and H–H–H angles of 152.9° and 146.7° for Al and Sc, respectively, demonstrate the similarity between the metallo reactions and the minor perturbation that either metal provides to the $H_2 + D$ exchange reaction with H–H distances of 0.911 Å (with the present computational approach) and H–H_b–H angle of 180.0° (see Table I, c and e, for the atomic coordinates and Table II, c and e, for a comparison of bond distances and angles). Both Al and Sc cause the H–H_b distance to increase relative to the free H_3 transition state by 0.16 Å and 0.10 Å, respectively.

The calculated activation energetics provide the major difference between the fragment three-electron case, the group 3 case, and the group 13 case (see Figure 7). The barrier for the aluminum case is 32.2 kcal/mol higher than for the scandium case. This difference is explained in terms of the better directionality afforded the transition metal d orbital (as shown in Figures 5d and 6d above) and the more favorable radical orbital energy match for the scandium system (see below). The calculated activation energy for the Sc case is only slightly different from that previously reported by Steigerwald and Goddard[4] (see the Calculational Details section below for a discussion of this difference) and is 4.6 kcal/mol *lower* than for the $H_2 + H$ case reported above. That is, Cl_2Sc actually *stabilizes* the transition state for the $H_2 + D$ exchange reaction (which has a calculated barrier of 14.4 kcal/mol with the present basis set and wave function). The Cl_2Al fragment is found to *destabilize* the transition state for the $H_2 + D$ exchange reaction.

In addition to the better directionality afforded the transition metal d orbital, the interacting fragment orbitals of Cl_2Al and Cl_2Sc are at substantially different energy (see Figure 8) and hence interact differently with the H atom of the reactant and the σ_u radical orbital of the H_3 transition state. The Cl_2Al radical orbital does not have a good energy match with either the reactant hydrogen atom radical orbital or the σ_u radical orbital of the H_3 transition state (see Figure 8a). Conversely the Cl_2Sc radical orbital *does* have a significantly better energy match with the σ_u

Table I. Molecular Coordinates and CI Total Energies[a]

atom	X	Y	Z	atom	X	Y	Z
			(a) $CH_3(H)CH_3$ Saddle Point CI Total Energy = −79.737 512				
H1	0.0	0.000 858 579	0.0	H4	0.900 474 716	0.519 598 467	−1.624 277 84
C1	0.0	0.000 039 071	−1.336 600 89	H5	0.900 474 716	0.519 598 467	1.624 277 84
C2	0.0	0.000 039 071	1.336 600 89	H6	−0.900 474 716	0.519 598 467	−1.624 277 84
H2	0.0	−1.040 091 80	−1.622 327 44	H7	−0.900 474 716	0.519 598 467	1.624 277 84
H3	0.0	−1.040 091 80	1.622 327 44				
			(b) Cl_2AlH CI Total Energy = −1161.567 288				
Al	0.0	0.0	0.791 967 289	Cl2	1.857 203 14	0.0	−0.334 671 848
Cl1	−1.857 203 14	0.0	−0.334 671 848	H	0.0	0.0	2.357 436 82
			(c) Cl_2AlH_3 Saddle Point CI Total Energy = −1162.651 567				
Al	0.0	0.0	0.674 622 474	H1	0.0	0.0	2.357 436 82
Cl1	−1.913 292 23	0.0	−0.348 063 754	H2	0.0	−1.039 869 03	2.034 414 07
Cl2	1.913 292 23	0.0	−0.348 063 754	H3	0.0	1.039 869 03	2.034 414 07
			(d) Cl_2ScH CI Total Energy = −965.658 779				
Sc	0.0	0.0	0.570 279 886	Cl2	2.140 057 45	0.0	−0.394 630 966
Cl1	−2.140 057 45	0.0	−0.394 630 966	H	0.0	0.0	2.325 665 18
			(e) Cl_2ScH_3 Saddle Point CI Total Energy = −966.794 493				
Sc	0.0	0.0	0.559 880 747	H1	0.0	−0.968 605 168	2.169 918 35
Cl1	−2.124 708 81	0.0	−0.451 630 808	H2	0.0	0.0	2.459 309 33
Cl2	2.124 708 81	0.0	−0.451 630 808	H3	0.0	0.968 605 168	2.169 918 35
			(f) Cl_2AlCH_3 Saddle Point CI Total Energy = −1200.620 403				
Al	0.0	0.012 721 436	0.463 733 142	H1	0.0	−1.027 906 37	2.783 518 82
Cl1	−1.843 114 34	−0.002 992 889	−0.348 063 754	H2	−0.880 557 264	0.485 377 638	2.811 637 99
Cl2	1.843 114 34	−0.002 992 889	−0.348 063 754	H3	0.880 557 264	0.485 377 638	2.811 637 99
C	0.0	−0.006 112 908	2.414 063 58				
			(g) $Cl_2AlCH_3(H)CH_3$ Saddle Point CI Total Energy = −1240.738 818				
Al	0.0	0.0	0.226 002 717	H2	0.0	−2.287 794 06	1.403 034 83
Cl1	−1.882 608 32	0.0	−0.877 941 446	H3	0.0	2.287 794 06	1.043 034 83
Cl2	1.882 608 32	0.0	−0.877 941 446	H4	−0.885 465 829	−1.621 702 30	2.377 916 36
C1	0.0	−1.473 893 62	1.771 503 17	H5	−0.885 465 829	1.621 702 30	2.377 916 36
C2	0.0	1.473 893 62	1.771 503 17	H6	0.885 465 829	−1.621 702 30	2.377 916 36
H1	0.0	0.0	1.892 590 29	H7	0.885 465 829	1.621 702 30	2.377 916 36
			(h) Cl_2ScCH_3 CI Total Energy = −1004.710 546				
Sc	0.0	−0.000 666 974	0.286 985 845	H1	0.0	1.016 622 60	2.847 365 60
Cl1	−1.913 292 23	0.000 336 788	−0.718 509 088	H2	0.0	−0.502 239 824	2.841 484 88
Cl2	1.913 292 23	0.000 336 788	−0.718 509 088	H3	0.0	−0.502 239 824	2.841 484 88
C	0.0	−0.000 510 818	2.451 601 02				
			(i) $Cl_2ScCH_3(H)CH_3$ Saddle Point CI Total Energy = −1044.882 757				
Sc	0.0	0.0	0.136 493 817	H2	0.0	−2.206 417 81	1.146 101 32
Cl1	−2.108 590 49	0.0	−0.945 394 775	H3	0.0	2.206 417 81	1.146 101 32
Cl2	2.108 590 49	0.0	−0.945 394 775	H4	−0.883 055 250	−1.612 927 57	2.533 014 70
C1	0.0	−1.437 376 42	1.930 251 56	H5	−0.883 055 250	1.612 927 57	2.533 014 70
C2	0.0	1.437 376 42	1.930 251 56	H6	0.883 055 250	−1.612 927 57	2.533 014 70
H1	0.0	0.0	1.989 722 97	H7	0.883 055 250	1.612 927 57	2.533 014 70

[a] Coordinates are in Å and energies in hartrees.

radical orbital of the H_3 transition state than with the reactant hydrogen atom radical orbital; hence for the Sc system the transition state is preferentially *stabilized* with respect to the reactant (see Figure 8b).

C. Methane Exchange. As was reported above for hydrogen exchange, for the methane exchange reaction the three predominantly C and bridging H (H_b) orbitals are virtually identical for the scandium and aluminum systems (see Figures 9 and 10, a–c) and are quite similar to those of the $CH_3 + CH_4$ system (compare Figures 9 and 10, a–c, with Figure 4, d–f). The greater directionality of the d orbital over the p orbital is apparent from a comparison of Figures 9d and 10d).

As expected from the comparison of valence orbitals, the geometries for the three transition states are quite similar. The C–H_b distances of 1.48 Å and 1.44 Å and C–H_b–C angles of 170.6° and 175.3° for Al and Sc, respectively, demonstrate the similarity in the reactions and the minor perturbation that either metal provides to the $CH_3 + {}^{13}CH_4$ exchange reaction with a C–H_b distance of 1.34 Å and an C–H_b–C angle of 180.0° (see Table I, g and i, for the atomic coordinates and Table II, g and i, for a comparison of bond distances and angles). As was seen for hydrogen exchange, both Al and Sc cause the C–H_b distance to increase relative to the free transition state (by 0.14 Å and 0.1 Å, respectively) by roughly the same amounts (as discussed above for hydrogen exchange, the increases were 0.16 Å and 0.1 Å). For Cl_2ScCH_3 we find a perfectly conventional structure (in accord with experimental work[1c] on $Cp^*_2ScCH_3$). The calculated Sc–C distance is 2.17 Å; the experimental Sc–C distance for $Cp^*_2ScCH_3$ is 2.243 (11) Å. The three Sc–C–H angles are all nearly 111°. The Sc–C–H angle for the H in the equatorial plane of the wedge is different from the other two (0.3° larger) as there were not any equivalence constraints applied *but* there is no evidence for an agostic interaction for this system. This description is consistent with a previous study by Williamson and Hall for Cl_3TiCH_3.[24]

As with the hydrogen exchange process, the calculated activation energetics provide the major difference between the group 3 and group 13 cases and the fragment three-electron system (see Figure 11). The barrier for the aluminum case is 33.7 kcal/mol higher than for the scandium case. As above, this difference is explained in terms of the better directionality afforded the transition metal d orbital (as shown in Figures 4d and 5d above).

For this case the Cl_2Sc fragment destabilizes the transition state for the $CH_3 + CH_4$ exchange reaction by 2.9 kcal/mol (calculated barrier of 25.1 kcal/mol with the present basis set and wave

(24) Williamson, R. L.; Hall, M. B. *J. Am. Chem. Soc.* **1988**, *110*, 4428.

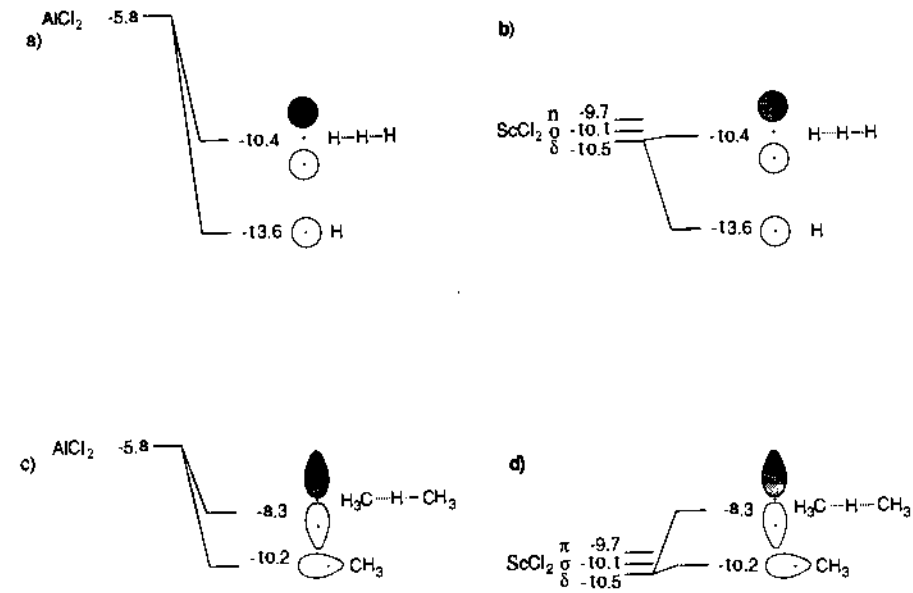

Figure 8. Correlation diagram relating the Cl_2Al, Cl_2Sc, H, and H_t fragment one-electron orbital energies (in eV) obtained from restricted Hartree–Fock wave functions: (a) the interactions between Cl_2Al and H and H_2, (b) the interactions between Cl_2Sc and H and H_2, (c) the interactions between Cl_2Al and CH_3 and C_2H_7, (d) the interactions between Cl_2Sc and CH_t and C_2H_7.

Table II. Major Bond Distances and Bond Angles[a]

	(a) $CH_t(H)CH_2$ Saddle Point		
H_b–C	1.337	C–H_b–C	179.93
C–H	1.079	H_b–C–H	105.4
	(b) Cl_2AlH		
Al–Cl	2.172	H–Al–Cl	121.24
Al–H	1.551		
	(c) Cl_2AlH_t Saddle Point		
Al–Cl	2.169	Cl–Al–H_b	118.13
Al–H	1.712	H–Al–H_b	37.41
Al–H_b	1.683	H–H_b–H	152.9
H–H_b	1.070		
	(d) Cl_2ScH		
Sc–Cl	2.348	H–Sc–Cl	114.27
Sc–H	1.755		
	(e) Cl_2ScH_t Saddle Point		
Sc–Cl	2.169	Cl–Sc–H_b	111.61
Sc–H	1.879	H–Sc–H_b	31.03
Sc–H_b	1.899	H–H_b–H	146.7
H–H_b	1.011		
	(f) Cl_2AlCH_t		
Al–Cl	2.182	C–Al–Cl	122.37
Al–C	1.950	Al–C–H_p	110.43
C–H	1.085	Al–C–H	111.25
	(g) $Cl_2AlCH_3(H)CH_3$ Saddle Point		
Al–Cl	2.182	Cl–Al–H_b	120.39
Al–C	2.136	C–Al–H_b	43.64
Al–H_b	1.667	C–H_b–C	170.6
C–H_b	1.479	Al–C–H_p	91.81
C–H_p	1.092	Al–C–H	119.95
C–H	1.083		
	(h) Cl_2ScCH_t		
Sc–Cl	2.365	C–Sc–Cl	115.16
Sc–C	2.165	Sc–C–H_p	111.27
C–H	1.090	Sc–C–H	110.97
	(i) $Cl_2ScCH_3(H)CH_3$ Saddle Point		
Sc–Cl	2.370	Cl–Sc–H_b	117.16
Sc–C	2.299	C–Sc–H_b	38.71
Sc–H_b	1.853	C–H_b–C	175.3
C–H_b	1.439	Sc–C–H_p	83.15
C–H_p	1.098	Sc–C–H	122.37
C–H	1.083		

[a] Distances are in Å and angles in deg.

function), and Cl_2Al destabilizes the transition state for the $CH_3 + CH_3D$ exchange reaction by 36.6 kcal/mol. In addition to the better directionality afforded the transition metal d orbital, the interacting fragment orbitals of Cl_2Al and Cl_2Sc are at substantially different energy (see Figure 8, c and d). The Cl_2Al radical orbital does not have a particularly good energy match with either the reactant methyl radical orbital or the radical orbital of the transition state (see Figure 8c). Conversely, the Cl_2Sc radical orbital does have a better energy match with the reactant methyl radical orbital than the transition state radical orbital, thus destabilizing the transition state (see Figure 8d).

It should be noted that substitution of the chloride ligand set with a pair of cyclopentadienyl ligands will raise the d levels by several electron volts (for X_2Ti the lowest d level is raised from −14.0 eV for X = Cl to −8.9 eV for X = Cp). This rise in orbital energy will certainly change the methane exchange reaction from being a destabilized case to being a stabilized case. Experimentally the methane exchange reaction for M = Sc and X = pentamethylcyclopentadienyl (Cp^*) occurs quite rapidly.

IV. Selective Stabilization and Destabilization of Transition States

Based on several previous theoretical studies as well as the present work, we feel confident that the discussion in section II above is, in fact, general. Four-center 2 + 2 reactions involving a single metal center are, electronically, minor perturbations on the analogous three-center radical plus bond reactions. In fact, we hypothesize that the endo- or exothermicity of these reactions as well as the height of the barriers connecting reactants and products can be affected by the energetic position of the metal orbitals on the ML_n fragments. That is, for the general four-center 2 + 2 reaction discussed above in section II, if there is a single dominant metal–ligand bonding interaction in the reactant between M and C, in the product between M and A, and along the reaction coordinate between M and the radical orbital antisymmetrically delocalized over centers A and C, then raising or lowering the metal orbital energies can strengthen or weaken the interactions between the metal and the reacting fragment orbitals.

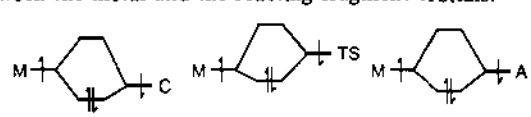

For example, if the orbital energy diagram for a given reaction is as indicated above, that is, the organic fragment radical orbital

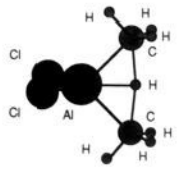

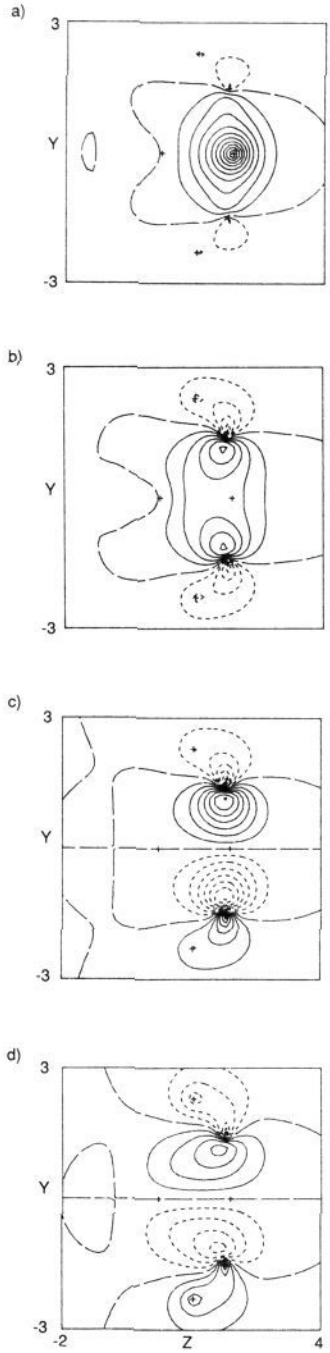

Figure 9. Contour plots of the GVB orbitals defining the one-electron orbitals of the $CH_4 + Cl_2AlCH_3$ transition state. The plotting plane contains the bridging hydrogen, both carbons, and aluminum. The solid contours define positive orbital amplitude (spaced 0.05 au), the dashed contours define negative orbital amplitude, and the long dashed lines define nodal lines: (a) the H_b σ one-electron orbital (of the first singlet coupled pair), (b) the symmetrically delocalized σ one-electron orbital (of the first singlet coupled pair), (c) the antisymmetrically delocalized σ one-electron orbital (of the second singlet coupled pair), (d) the antisymmetrically delocalized σ one-electron orbital (of the second singlet coupled pair) more delocalized onto Al.

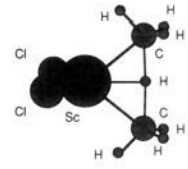

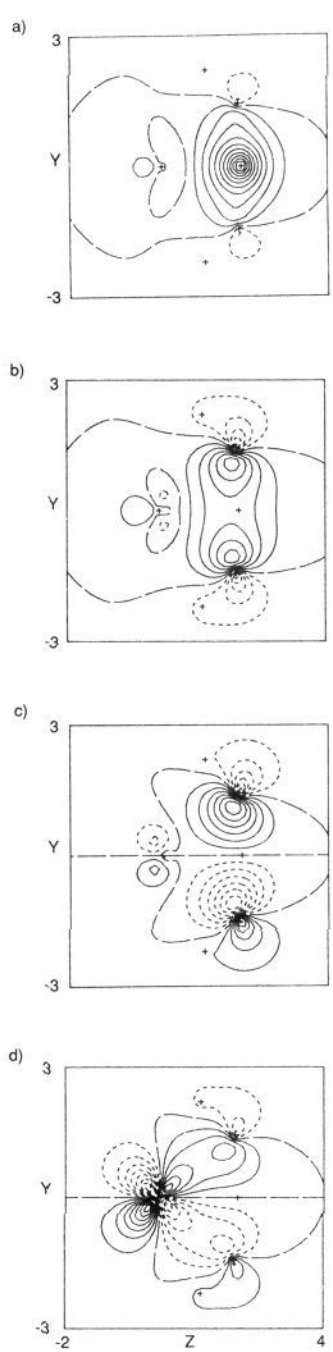

Figure 10. Contour plots of the GVB orbitals defining the one-electron orbitals of the $CH_4 + Cl_2ScCH_3$ transition state. The plotting plane contains the bridging hydrogen, both carbons, and scandium. The solid contours define positive orbital amplitude (spaced 0.05 au), the dashed contours define negative orbital amplitude, and the long dashed lines define nodal lines: (a) the H_b σ one-electron orbital (of the first singlet coupled pair), (b) the symmetrically delocalized σ one-electron orbital (of the first singlet coupled pair), (c) the antisymmetrically delocalized σ one-electron orbital (of the second singlet coupled pair), (d) the antisymmetrically delocalized σ one-electron orbital (of the second singlet coupled pair) more localized on Sc.

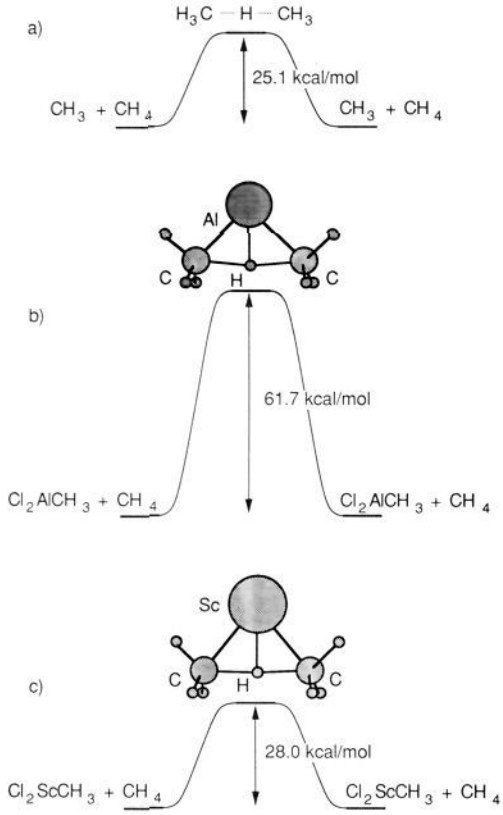

Figure 11. The reaction energy diagrams for methane exchange processes: (a) the free $CH_3 + CH_4$ case; (b) the $Cl_2AlCH_3 + CH_4$ case; (c) the $Cl_2ScCH_3 + CH_4$ case. The energies are obtained from the CI calculations.

at the transition state is at higher energy than the fragment radical orbital in C (the reactant) or A (the product), and if the metal fragment orbital of interest is below the organic fragment radical orbital at the transition state, then ligand or metal substitution that would raise the energy of the metal fragment orbital would decrease the height of the barrier and lower the activation energy for the reaction. This analysis of the stabilization of the transition state is analogous to standard orbital energy diagram analyses used to explain relative bond strengths.[25] The expression used to quantify the effect is

$$E_{stab} \propto S_{12}^2/|\epsilon_1 - \epsilon_2|$$

where E_{stab} is the stabilization energy afforded the lower energy level, S_{12} is the overlap between the two radical orbitals, and ϵ_1 and ϵ_2 are the orbital energies of the two radical orbitals.

For the specific cases discussed above ($ML_n = ScCl_2$), the methane exchange reaction demonstrates transition-state destabilization (by 2.9 kcal/mol), and the hydrogen exchange reaction demonstrates transition-state *stabilization* (by 4.6 kcal/mol). Comparison of the energy denominator terms for the reactants and transition states for these two reactions leads to the suggestion that the hydrogen exchange reaction should be stabilized more than the methane exchange reaction is destabilized. The energy denominators for the H and H_3 radicals are 0.323 eV^{-1} and 10.0 eV^{-1}. The energy denominators for the CH_3 and C_2H_7 radicals are 3.33 eV^{-1} and 0.455 eV^{-1}. The ratio of differences (assuming constant overlap) would suggest that the hydrogen exchange reaction would be stabilized by ca. three times the amount that the methane exchange reaction is destabilized. In fact, we observe a differential effect of 1.6.

Comparison of the geometries of a series of four-center 2 + 2 transition states with the transition states for the analogous radical plus bond reactions[17-22] given in Figure 12 provides further support for the hypothesis that addition of a metal orbital and the fourth electron provides only a modest perturbation to the transition state for the analogous three-electron radical plus bond reaction. The major feature ascribed to the metal is the capacity for its participating d (or p for Al) orbital (the fourth orbital in the 2 + 2 reaction) to rehybridize through the mixing in of an additional, empty d (or p for Al) orbital. This rehybridization permits retention of overlap with the third or radical orbital of the bond plus radical reaction. For this analysis the Ti–C σ bond in the carbene is deemed equivalent to a C–H σ bond in the analogous methyl moiety.

The orbital energies given in Figure 13 for the third (or radical) orbital calculated at the transition state geometries for radical plus bond reactions from the literature[17-22] as well as the radical orbitals for the reactants and products demonstrate the variability of the fragment radical orbital energies along a reaction coordinate as well as the range of the fragment radical orbital energies among reactions. For example, for H_2 plus H the hydrogen atomic orbital energy is −13.6 eV and the SO-GVB radical orbital energy for the transition state is −11.5 eV (a difference of 2.1 eV). The effect of metal and/or ligand perturbations on energetic position of the fragment metal orbitals is as shown in Figure 14 for group 4 halides. Within this rather limited set there is a variation of 6.2 eV; in fact, it spans the range of organic fragment orbital energies discussed above. A systematic study of the effect of metal and/or ligand substitution on the overall reaction energetics for the above-discussed reactions would provide data for confirmation or modification of our hypothesis.

V. Conclusions

We have found that group 13 metals, specifically aluminum, can participate in the same unique reactivity patterns (attributed to quite small activation energetics for four-center 2 + 2 reactions) that have been observed for early transition metals. In agreement with Rooney's hypothesis, we find that an empty p orbital can rehybridize with a bonding p orbital to permit four-center 2 + 2 reactions to occur with relatively low activation energies. However, the greater directionality of a d orbital permits the reactions to occur with substantially lower barriers for the transition metal cases (for hydrogen exchange the Al barrier is 32.2 kcal/mol higher than for Sc; for methane exchange the Al barrier is 33.7 kcal/mol higher than for Sc). Further, we have presented computational evidence for the hypothesis that metal fragment orbitals can be tuned to either stabilize transition states of preferred reactions or destabilize transition states for pathways that are not desired. We have calculated a barrier for methane exchange of 28.0 kcal/mol for $Cl_2Sc(CH_3) + CH_4$. Further, we determined the methyl plus methane exchange process to occur with a barrier of 25.1 kcal/mol.

VI. Calculational Details

A. Basis Sets and Effective Potentials. All of the calculations reported here were carried out using Cartesian Gaussian basis sets. For Al and Cl[26] effective potentials were used to replace the core electrons allowing self-consistent orbital optimization to be carried out only for the valence electrons. For Sc[27] an effective potential was used to replace the 1s, 2s, and 2p orbitals again reducing the number of functions for the self-consistent orbital optimization. For geometry optimizations a (7s,4p/3s,3p) basis set was used for carbon.[28] A (6s/3s) basis, unscaled, was used for the hydrogens in H_2 or bound to the metal.[29] A (4s/2s) basis, scaled, was used for the hydrogens in methyl and methane not participating in the reaction.[29] For the final series of calculations to determine the energetics, the Dunning–Huzinaga[29] valence double-ζ carbon basis set was used, augmented with a set of d Gaussians ($\zeta = 0.75$).[30] The unscaled triple ζ hydrogen basis was augmented with a single set of p Gaussians ($\zeta = 0.6$) for the final series of calculations. For chlorine, a valence minimum basis (3s,3p/1s,1p)[25] was used for all calculations. For

(25) Albright, T. A.; Burdett, J. K.; Whangbo, M.-H. *Orbital Interactions in Chemistry*; Wiley: New York, 1985.

(26) Rappé, A. K.; Smedley, T. A.; Goddard, W. A. *J. Phys. Chem.* **1981**, *85*, 1662–1666.

(27) Hay, P. J.; Wadt, W. R. *J. Chem. Phys.* **1985**, *82*, 270–283.

(28) Rappé, A. K.; Goddard, W. A. Manuscript in preparation.

(29) Huzinaga, S. *J. Chem. Phys.* **1965**, *42*, 1293.

(30) Dunning, T. H.; Hay, P. J. In *Modern Theoretical Chemistry: Methods of Electronic Structure Theory*; Schaefer, H. F., III, Ed.; Plenum Press: New York, 1977; Vol. 3, Chapter 1, pp 1–27.

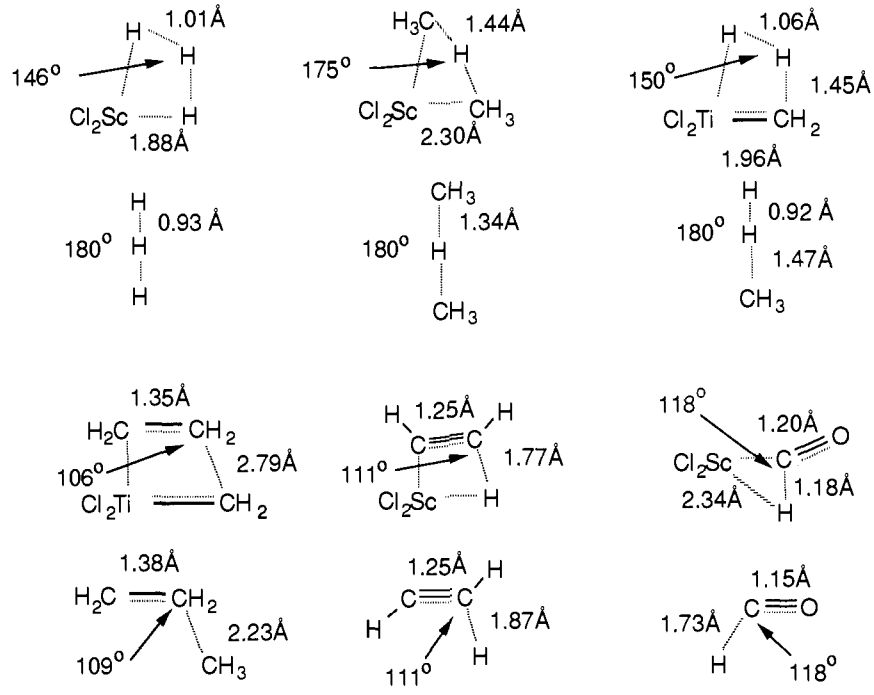

Figure 12. Comparison of four-center 2 + 2 metallo transition states with the analogous three-center bond plus radical transition states.

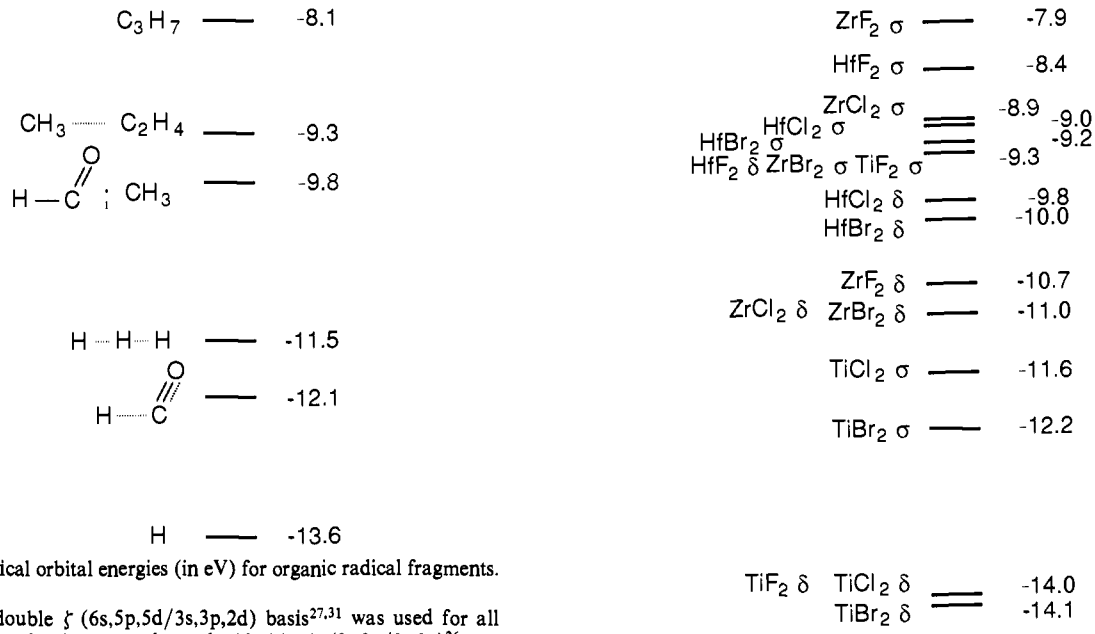

Figure 13. Radical orbital energies (in eV) for organic radical fragments.

Figure 14. Radical orbital energies (in eV) for metallic diradical fragments.

Sc, a valence double ζ (6s,5p,5d/3s,3p,2d) basis[27,31] was used for all calculations. For aluminum, a valence double ζ basis (3s,3p/2s,2p)[26] was used for the geometry optimizations and was augmented by a set of d functions ζ = 0.25 for the final energy calculations.

B. Wave Functions. The geometries of the stationary points were generated with analytic gradient techniques using restricted Hartree–Fock wave functions. For the final optimized geometries, GVB(2/4) wave functions[32] were obtained and CI calculations[33] were performed consisting of RCI quadruples plus a Pol(2/1)-CI[34] including the GVB orbitals and the entire virtual space. For each transition state structure the four active electrons were correlated. For each of the reactants, the single participating bond was correlated.

As mentioned above, Steigerwald and Goddard[4] have previously studied the $Cl_2ScH + H_2$ transition state. They optimized the geometry of the transition state using analytic Hartree–Fock gradients but kept the Cl_2Sc fragment fixed at the geometry of Cl_2ScH. As can be seen by a comparison of Table I, d and e, this is not a bad approximation. Further, they did not use an effective core potential on Sc. The $H–H_b$ distance obtained by Steigerwald and Goddard was 1.014 Å compared to our value of 1.011 Å. The $H–H_b–H$ angle obtained by Steigerwald and Goddard was 149° compared to our value of 146.7°. The Sc–H distances obtained for Steigerwald and Goddard for Cl_2ScH and Cl_2ScH_3 were 1.78 Å and 1.887 Å, respectively, our distances are 1.755 Å and 1.879 Å. The agreement is good and is indicative of the validity of the effective core potential. The wave functions used to determine the barrier heights are quite similar except (as discussed above) we augmented the hydrogen basis with a set of p functions. This basis set difference yields the major difference between the two efforts. Our barrier height of 9.8 kcal/mol is about one-half the height of the barrier obtained by Steigerwald and Goddard of 17.7 kcal/mol.

Acknowledgment. This work was partially supported by NSF Grant CHE-8405399. A.K.R. acknowledges partial support of this research by the Union Carbide Innovation Recognition program.

(31) Rappé, A. K.; Smedley, T. A.; Goddard, W. A. *J. Phys. Chem.* **1981**, *85*, 2607–2611.
(32) Bobrowicz, F. W.; Goddard, W. A. In *Electronic Structure Theory*; ref 30, Chapter 4, pp 79–127.
(33) Shavitt, I. In ref 3, Chapter 6, pp 189–275.
(34) Hay, P. J.; Dunning, T. H. *J. Chem. Phys.* **1976**, *64*, 5077.